



# The effect of MBS on the heat resistant, mechanical properties, thermal behavior and rheological properties of PLA/EVOH blend

Yanping Hao<sup>1</sup> · Huili Yang<sup>1</sup> · Hongwei Pan<sup>1</sup> · Xianghai Ran<sup>1</sup> · Huiliang Zhang<sup>1</sup>

Received: 16 November 2017 / Accepted: 5 June 2018 / Published online: 11 July 2018  
© Springer Nature B.V. 2018

## Abstract

This work focuses on improve the mechanical properties of poly(lactic acid)/poly(ethylene-co-vinyl alcohol) (PLA/EVOH) blend and simultaneously remained a high Vicat softening temperature (VST) using appropriate contents of methyl methacrylate–butadiene–styrene copolymer (MBS) via simple melt blending. The effects of MBS on the heat resistant, mechanical properties, thermal properties and rheological behavior were examined in detail with various techniques. The VST of neat PLA significantly increased to 159 °C from 66.8 °C after blending with 50 wt% EVOH. However, the VST was gradually decreased with increasing MBS content but were still much higher than that of neat PLA. On the basis of the tensile and impact tests results, PLA/EVOH/MBS blends showed a considerably higher elongation at break and impact strength. For all PLA/EVOH/MBS blends, the thermal stability was increased compared than that of PLA/EVOH blend without MBS. With increasing MBS content, the complex viscosity and storage modulus of PLA/EVOH blend increased, especially at low frequencies, indicating that MBS enhanced the chain entanglement in the PLA/EVOH matrix. In addition, the results Han curves and Cole–Cole plots indicated that the relaxation time was increased when MBS was added.

**Keywords** Poly(lactic acid) · Heat resistant · Mechanical properties · Thermal behavior · Rheological properties

## Introduction

Poly(lactic acid) (PLA) is an aliphatic and thermoplastic polyester that has attracted considerable attention because of its renewability, biodegradability, transparency, and mechanical properties [1–5]. Therefore, PLA is expected to replace polyethylene (PE), polystyrene (PS), and other traditional petroleum-based plastics in most applications. PLA has a broad potential for application in the manufacturing of containers, packaging materials, fabrics, and medical devices [6, 7]. However, there are some drawbacks, including its brittleness and poor heat resistance when applied to the temperature above its glass transition temperature. For example, PLA

products fabricated by extrusion, film blowing, or injection molding processes can only achieve a Vicat softening temperature of about 60 °C [8], and this relatively poor heat resistance restricts the application of PLA [9, 10]. Thus, traditional PLA is not sufficiently heat resistance for used in the manufacturing drinking cups for hot liquids, utensils, and other food-related containers.

Various methods have been explored to improve the heat resistance temperature (HDT) of PLA. One method is to incorporate heat-resistant reinforcing fillers into PLA to increase the HDT. Additions of wood fiber [11, 12], glass fiber [13], cellulose fiber [14], wheat straw [15, 16], corn stover and soy stalks [16] to PLA, were all noted to increase HDT; however, the improvement in HDT is limited (within 20 °C). Another method is to add a nucleating agent to increase the crystallinity and hence improve the heat resistance of PLA. Talc [17], montmorillonite [18], and bismaleimide [19] were studied as nucleating agents for PLA, and behaved differently in improving the HDT of PLA. While addition of 9.1 wt% talc brought about an increase of 1 °C in the HDT of PLA [17], incorporation of 8 wt% montmorillonite to PLA resulted in an increase of 28 °C in HDT [18]. A further increment is limited mainly due to aggregation of the nucleating agents. The third

✉ Xianghai Ran  
ranxh@ciac.ac.cn

✉ Huiliang Zhang  
hlzhang@ciac.ac.cn

<sup>1</sup> Key Laboratory of Polymer Ecomaterials, Chinese Academy of Sciences, Changchun Institute of Applied Chemistry, Changchun 130022, People's Republic of China

method is to blend PLA with highly heat-resistant polymers, which has proved to be more effective. Polycarbonate (PC) [20], poly(methyl methacrylate) [21], and poly(acrylonitrile-co-butadiene-co-styrene) [22] were employed to blend with PLA to increase its HDT.

EVOH is a semi-crystalline thermoplastic copolymer with excellent barrier properties, high resistance to oil and higher Vicat softening temperature. Also, EVOH is a bio-compatible polymer and easy to process, thus it has attracted interest in academia and industry as well. EVOH is both hydrophilic and hydrophobic in nature due to the presence of alcohol groups and ethylene repeating units respectively. Previous researchers have used EVOH to improve the HDT of PLA. Liu et al. reported that the PLA/EVOH/TAIC blends with such a crosslinked network have dramatically enhanced the HDT values, as high as 140 °C [23].

In this work, PLA/EVOH blend containing 50 wt% EVOH is expected to exhibit a high VST. EVOH was purposely selected because it displays a higher VST of 164 °C (measured in our laboratory). Furthermore, the melting point of EVOH (around 180 °C) is close to that of PLA, making it suitable for blending with PLA. In addition, methyl methacrylate–butadiene–styrene copolymer (MBS) had a soft core (butadiene–styrene copolymer) and a hard shell (PMMA) and it used as an impact modifier to improve the mechanical properties of PLA in our previous research [24]. Thus, MBS was added in order to improve the mechanical properties of PLA/EVOH blend and simultaneously remained a high VST. The effect of MBS content on heat resistant, mechanical properties, thermal behavior and rheological properties of the PLA/EVOH blend were investigated.

## Experimental

### Materials

PLA (4032D) used in this study comprising around 98% L-lactide was a commercial product of Natureworks Co. Ltd., USA. It had molecular weight ( $M_w$ ) of 250,000 g/mol and polydispersity of 1.70 (by GPC analysis). MBS, trademark: B-625, was purchased from Kaneka Corporation, Japan. EVOH, trademark: F171B, was purchased from Kuraray Co., Ltd., Japan.

### Sample preparation

The weight ratio of the PLA/EVOH blend was fixed at 50/50 w/w. Moreover, MBS was added to this blend at various loadings (5, 9, 13 and 17 phr). All samples were designated PLA, P-E0, P-E5, P-E9, P-E13 and P-E17, respectively. The PLA, EVOH and MBS components were first dried in a vacuum oven at 80 °C for 12 h to remove the moisture

absorbed. Then they were melted and mixed in a Haake rheomix 600 internal mixer for 5 min. The temperature of the mixer was maintained at 190 °C, and the roller speed was 60 rpm. After mixing, all samples were cut into small pieces and were hot-pressed at 190 °C, a hold pressure of 6 MPa and a hold time of 5 min, followed by quenching to room temperature between two thick metal blocks kept at room temperature. A template frame was used to ensure a constant sheet thickness of 4.0 mm for impact tests and 1.0 mm for tensile tests, and care was taken to ensure the same thermal history for all sheets.

### Characterization

A heat deformation Vicat temperature testing machine WKW-300 (Institute of Intelligence testing machine, Changchun, China) was used to obtain the Vicat softening temperature of all samples with the size of 12 mm × 12 mm × 3.3 mm. The samples were heated from room temperature in silicon oil medium under constant load of 1000 g with a heating rate of 2 °C/min according to GB/T1633-2000 (China).

The uniaxial tensile tests were carried out at room temperature on an 1121 testing machine (Instron Corporation, USA). Specimens (20 mm × 4 mm × 1 mm) were cut from the previously compression-molded sheet into a dumbbell shape. The measurements were conducted at a cross-head speed of 10 mm/min at room temperature according to ASTM D638-2008. At least five runs for each sample were measured, and the results were averaged.

Notched Izod impact tests were performed at room temperature according to ASTM D256-2010 on an impact testing machine (Institute of Intelligence testing machine, Changchun, China). The samples with dimensions 63.2 mm × 12.0 mm × 4.0 mm were obtained from compression-molded specimens. The notch was milled in having a depth 2.54 mm, an angle of 45° and a notch radius of 0.25 mm.

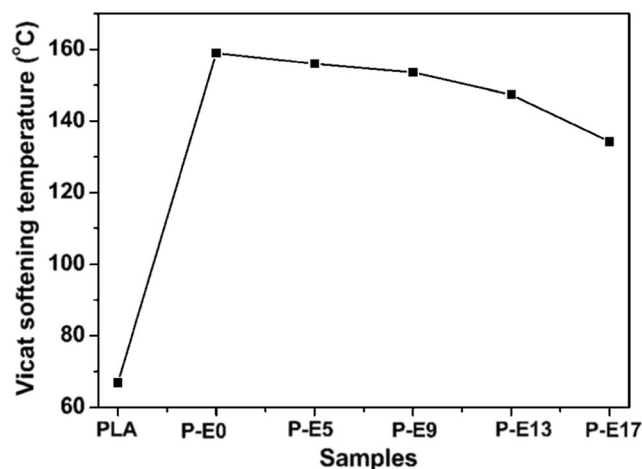


Fig. 1 Effects of the MBS content on the VST of PLA/EVOH blend

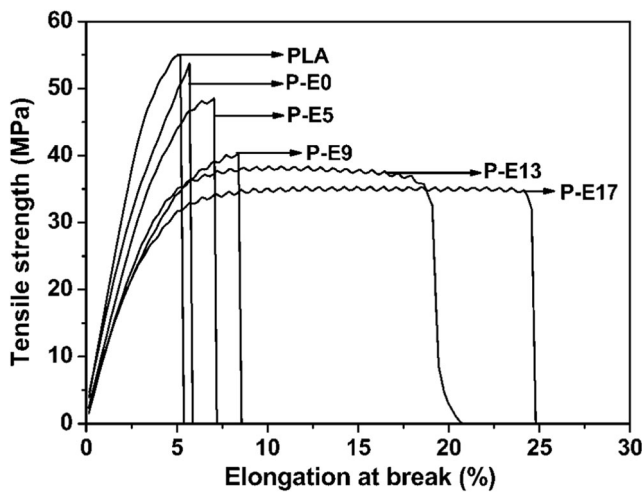


Fig. 2 Stress-strain curves of all samples

Thermal properties of all samples were studied by differential scanning calorimetry (DSC) (TA Instruments Co., DSC, Q20, USA) on the specimens sliced from compression molded samples. Samples (about 5–8 mg) were placed and sealed in aluminum pans. All samples were then heated first from 20 up to 220 °C at 10 °C/min (the first heating scan) and held at 220 °C for 3 min to eliminate their previous thermal history. Following that the samples were cooled to 20 °C at the same rate and then heated again finally (the second heating scan).

The thermal stability of all samples was measured by thermogravimetric analysis (TGA, Perkin-Elmer TGA-7, USA) simultaneous thermal analysis instrument. All samples with weight of  $10 \pm 0.2$  mg were heated from room temperature to 600 °C at 10 °C/min under nitrogen.

PLA/EVOH blend without MBS and PLA/EVOH blend with 9 phr MBS were subjected to the TGA in a nitrogen atmosphere. The experiments were conducted at five different heating rates (5, 10, 20, 30 and 40 °C/min) from room temperature to 600 °C.

Rheological measurements of all samples were conducted with the rheometer (TA Instruments Co., AR 2000ex, USA) at 190 °C. Frequency sweep for all samples was carried out under nitrogen using 25-mm plate-

plate geometry. The gap distance between the parallel plates was 0.9 mm for all tests. The sheet samples were about 1.0 mm in thickness. The angular frequency range used during testing was 0.1–100 rad/s.

The morphology of the fractured surface which was prepared under liquid nitrogen was observed using a field emission scanning electron microscopy (SEM) (XL-30 ESEM FEG, FEI Co., USA). The surface of the samples was coated with a thin layer of gold prior to the measurement.

## Results and discussion

### Vicat softening temperature

Because VST is a key property in the selection of materials for commercial and industrial applications, improving a composite's VST could open up new uses for PLA. Fig. 1 shows the values of VST for all samples. Interestingly, an obvious increase of VST was observed when EVOH was added into PLA. For instance, the VST of neat PLA increased from 66.8 °C to 159 °C after blending with 50 wt% EVOH. However, the VST was gradually decreased with increasing MBS content. For example, the VST of PLA/EVOH blend with 17 phr MBS reached the minimum value of 134.3 °C but was still much higher than that of PLA. In general, there are three options to increase the heat resistance of a polymer: increasing the  $T_g$ , increasing the crystallinity, and reinforcing [25]. For the PLA/EVIOH/MBS blends, the improvement of VST might be due to that the addition of EVOH and MBS hindered the movements of polymer chains and therefore delayed the deformation to higher temperature. In addition, it was noteworthy that the VST of all samples were higher than the VST of 82 °C typical of polystyrene that was usually used in the production of plates and cups for hot food or beverages. Thus, the addition of EVOH and MBS was significant to enlarge the application field of PLA materials and easy to be employed in practical processing.

Table 1 Mechanical properties of neat PLA and PLA/EVOH/MBS blends

Samples	Young's Modulus (MPa)	Tensile strength (MPa)	Elongation at break (%)	Impact strength (kJ/m <sup>2</sup> )
PLA	1504 ± 47	55.1 ± 4.2	5.3 ± 0.3	3.0 ± 0.2
P-E0	1321 ± 17	53.7 ± 3.6	5.9 ± 0.1	4.8 ± 0.3
P-E5	1096 ± 21	48.5 ± 2.0	9.8 ± 0.4	5.6 ± 0.2
P-E9	1042 ± 22	40.3 ± 1.8	8.6 ± 0.2	6.3 ± 0.2
P-E13	971 ± 19	38.4 ± 1.2	19.2 ± 1.2	7.6 ± 0.4
P-E17	951 ± 24	35.3 ± 1.5	24.7 ± 0.9	10.1 ± 0.6

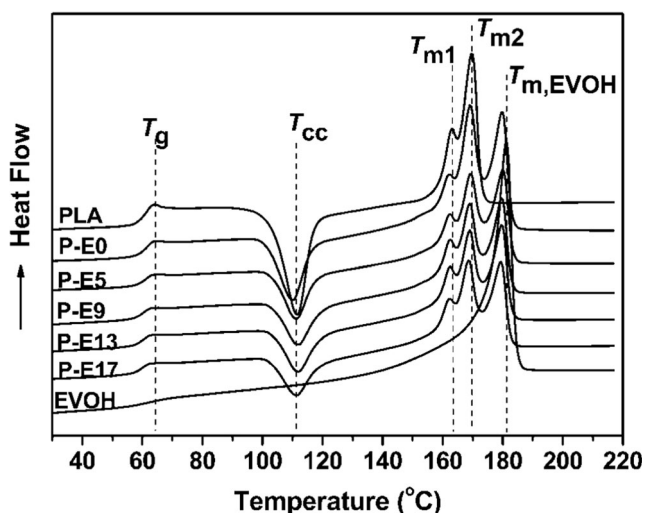


Fig. 3 DSC heating curves of all samples with a heating rate of 10 °C/min

### Mechanical properties

The goal of adding MBS to PLA/EVOH blend is to enhance plastic elongation and reduce brittleness. The stress-strain curves of all samples are shown in Fig. 2. It could be seen that PLA/EVOH blend without MBS content fractured at a lower tensile strain and no yield point was observed. The blends presented a yield point before the break and a subsequent plastic deformation which suggested that the addition of MBS was an effective means to improve the tensile toughness of PLA/EVOH blend. The tensile strength, Young's modulus, and elongation at break for all sample are shown in Table 1. It could be seen that PLA/EVOH blend without MBS content exhibited a tensile strength of 53.7 MPa, Young's modulus of 1321 MPa and an elongation at break of 5.9%. The PLA/EVOH blend with 17 phr MBS content had a higher value of elongation at break of 24.7%. However, the tensile strength and Young's modulus decreased when MBS was added, which was due to the elastomeric nature of the PB rubber phase in MBS. For example, the tensile strength and Young's modulus decreased to 35.3 MPa and 951 MPa when the fraction of MBS was 17 phr. The results indicated that the addition of MBS improved the ductility of PLA/EVOH blend.

**Table 2** Thermal properties of neat PLA and PLA/EVOH/MBS blends

Samples	$T_g$ (°C)	$T_{cc}$ (°C)	$\Delta H_{cc}$ (J/g)	$T_{m1}$ (°C)	$T_{m2}$ (°C)	$\Delta H_f$ (J/g)	$T_{onset,PLA}$ (°C)	$T_{max,PLA}$ (°C)
PLA	61.4	111.4	34.6	163.0	169.7	41.9	348.0	365.5
P-E0	61.6	110.1	20.6	161.9	168.9	24.4	308.1	344.5
P-E5	61.3	111.3	16.1	162.1	169.1	18.9	324.3	344.4
P-E9	61.3	111.6	18.3	162.4	168.9	22.9	331.1	350.7
P-E13	60.4	112.3	15.9	162.4	168.8	19.4	331.5	348.2
P-E17	60.1	111.7	15.0	162.1	168.5	19.4	327.5	349.2

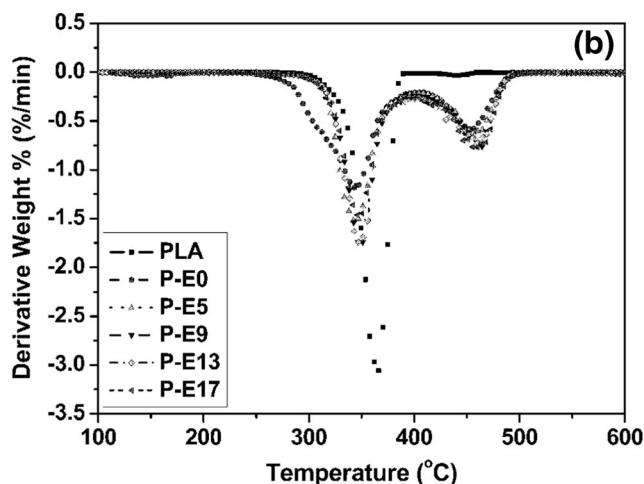
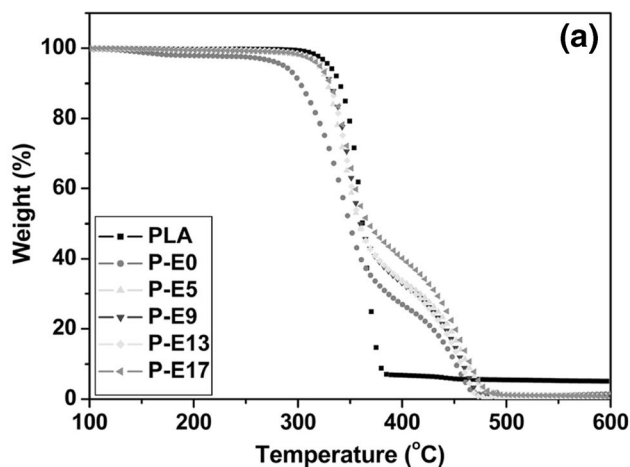


Fig. 4 Effect of MBS on the thermal stability of PLA/EVOH blend: a TGA and b DTG

Impact strength is a very important parameter to characterize the impact toughness and fracture resistance of materials. The impact strength of all samples is given in Table 1. The impact strength of PLA/EVOH blend without MBS content was about 3.1 kJ/m<sup>2</sup>, while the PBT/EVOH/MBS blends possessed a high notched impact strength. As shown in Table 1, it could be seen that the PLA/EVOH blend with 17 phr MBS achieved the highest notched impact strength of 10.1 kJ/m<sup>2</sup>. This result might be explained by that MBS could act as an elastomer to absorb the breaking energy during the Izod impact tests.

### Thermal behavior

Thermal behavior of neat PLA and PLA/EVOH/MBS blends were investigated by means of DSC and TGA. Figure 3 shows the DSC second heating traces of all samples after quenched from the molten state. The parameters for thermal behavior obtained from the heating run are listed in Table 2. As shown in Fig. 3, it was observed that the PLA/EVOH blend exhibited

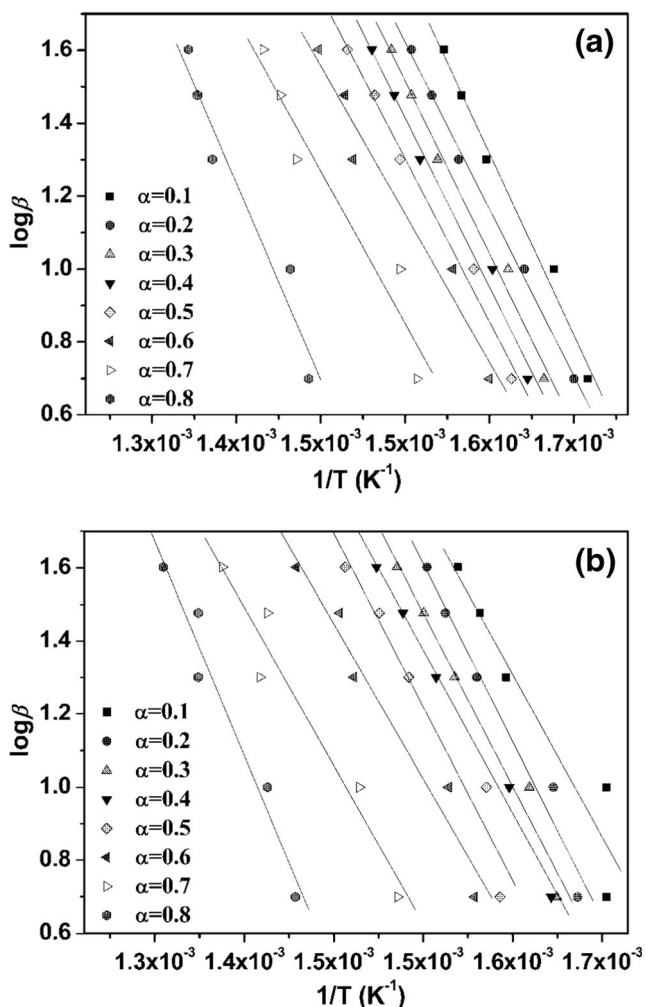


Fig. 5 Flynn–Wall–Ozawa plots at the following different weight losses of a P-E0 and b P-E9

a glass transition at 61.6 °C. The addition of MBS did not result in a marked change in the glass transition temperature of PLA. The heating curve of PLA/EVOH and PLA/EVOH/MBS blends displayed very distinct exothermic peaks and double melting peaks for cold crystallization temperature ( $T_{cc}$ ) and melting temperature ( $T_m$ ) respectively. The addition of MBS had little effect on  $T_{cc}$  and  $T_m$  values of PLA/EVOH/MBS blends when compared with that of PLA/EVOH blend, as shown in Table 2. Moreover, the melting peak of EVOH was observed at 180 °C. The heat of cold-crystallization ( $\Delta H_{cc}$ ) and the heat of melting ( $\Delta H_f$ ) for PLA decreased when MBS added in the PLA/EVOH blend, suggesting that the addition of MBS decreased the crystallinity of PLA.

The effect of the MBS on the thermal stability of PLA/EVOH blend were studied by thermogravimetry. The integral (TGA) and derivative (DTG) thermogravimetric curves provide information about the nature and extent of degradation of the polymeric materials. The TGA and DTG traces for all samples in nitrogen atmosphere are shown in Fig. 4. The thermal degradation behaviors of various samples were compared

Table 3 Activation energies of P-E0 and P-E9 by Flynn–Wall–Ozawa method

Samples	Conversion $\alpha$	r	$E\alpha$ (kJ/mol)	$\bar{E}\alpha$ (kJ/mol)
P-E0	0.1	0.9936	129.5	120.3
	0.2	0.9983	118.9	
	0.3	0.9939	122.9	
	0.4	0.9934	120.7	
	0.5	0.9940	116.1	
	0.6	0.9804	105.6	
	0.7	0.9681	108.7	
	0.8	0.9727	140.1	
P-E9	0.1	0.9549	115.6	121.8
	0.2	0.9859	126.7	
	0.3	0.9882	123.3	
	0.4	0.9958	116.1	
	0.5	0.9737	123.5	
	0.6	0.9789	107.9	
	0.7	0.9721	112.4	
	0.8	0.9786	149.1	

using the initial decomposition temperature ( $T_{onset}$ ) and the temperature of maximum rate of weight loss ( $T_{max}$ ) in order to understand the effects of MBS on the thermal degradation process of PLA. And the  $T_{onset}$  and  $T_{max}$  of PLA are illustrated in Table 2. In Figs. 4(a) and (b), it could be observed that neat PLA evidenced a one-stage weight loss during thermal decomposition, while PLA/EVOH and PLA/EVOH/MBS blends evidenced a two-stage weight loss. The first stage belonged to the degradation of PLA and the second stage was the degradation of EVOH. Neat PLA started to decompose at 348.0 °C ( $T_{onset}$ ). After that, the weight loss increased quickly, and the maximum degradation rate occurred at 365.5 °C ( $T_{max}$ ). The  $T_{onset}$  and  $T_{max}$  of PLA blended with EVOH alone that is, P-E0, it was shifted systematically to lower temperatures. However, the  $T_{onset}$  and  $T_{max}$  of PLA was shifted to higher temperature with the usage of MBS, as shown in Figs. 4(a) and (b). Thereby, the PLA/EVOH/MBS blends were more stable than PLA/EVOH blend without MBS.

The dynamic TGA method was a promising tool to unravel the mechanisms of physical and chemical processes that occur during polymer degradation. Generally, for polymer degradation, all kinetic studies assume that the isothermal rate of conversion  $d\alpha/dt$  is proportional to the concentration of reacted material. The rate of conversion can be expressed by the following basic rate equation:

$$\frac{d\alpha}{dt} = k(T)f(\alpha) \tag{1}$$

where  $f(\alpha)$  and  $k(T)$  are function of conversion and temperature, respectively.

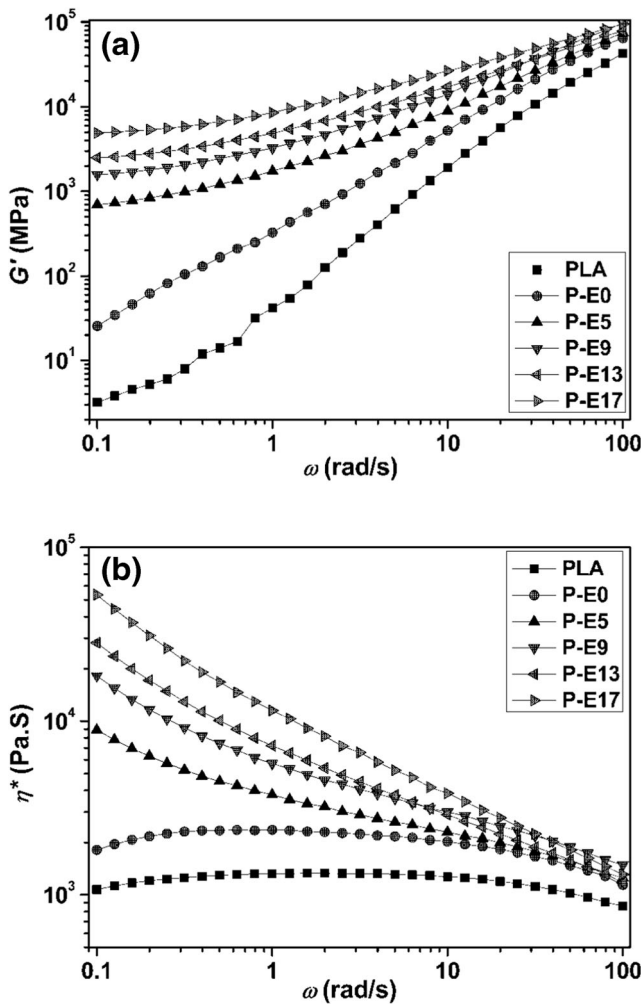


Fig. 6 a Dynamic storage modulus ( $G'$ ) and b complex viscosity ( $\eta^*$ ) versus angular frequency ( $\omega$ ) for all samples

$k(T)$  is often modeled successfully by the Arrhenius equation:

$$k(T) = A \exp\left(-\frac{E\alpha}{RT}\right) \quad (2)$$

where  $E\alpha$  is the pyrolytic decomposition activation energy,  $A$  the pre-exponential factor and  $R$  the gas constant.

$f(\alpha)$  depends on the particular decomposition mechanism. The simplest and most frequently used model for  $f(\alpha)$  in the analysis of TGA data is:

$$f(\alpha) = (1-\alpha)^n \quad (3)$$

where  $n$  is the order of reaction.

Insertion of Eqs (2) and (3) into Eq. (1) gives

$$\frac{d\alpha}{dt} = \beta \frac{d\alpha}{dT} = A(1-\alpha)^n e^{-\frac{E\alpha}{RT}} \quad (4)$$

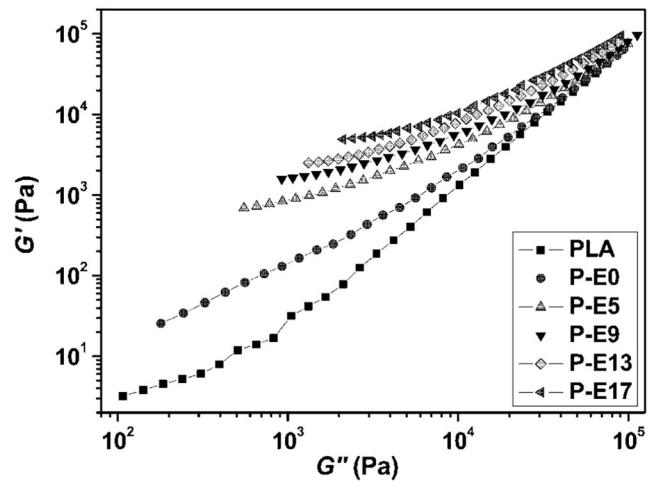


Fig. 7 Han plots of dynamic storage modulus ( $G'$ ) versus dynamic loss modulus ( $G''$ ) at 190 °C for all samples

Flynn-Wall-Ozawa method [26] Eq. (4) is integrated using Doyle's approximation [27], and the result of the integration after taking logarithms is:

$$\log F(\alpha) = \log \frac{AE\alpha}{R} - \log \beta - 2.315 - 0.4567 \frac{E\alpha}{RT} \quad (5)$$

Thus, it is used to determine the activation energy for given values of conversion. The activation energy for different conversion values can be calculated from a  $\log \beta$  versus  $1/T$  plot.

The thermal degradation kinetic analysis of PLA/EVOH blend without MBS content and PLA/EVOH blend with 9 phr MBS content were determined with Flynn-Wall-Ozawa method. The Flynn-Wall-Ozawa plots are shown in Fig. 5. Figures 5(a) and (b) showed that the fitting lines were straight lines with a good correlation coefficient  $r$ , which indicated the applicability of Flynn-Wall-Ozawa to the systems in the conversion range investigated. The  $E\alpha$  of samples are given in

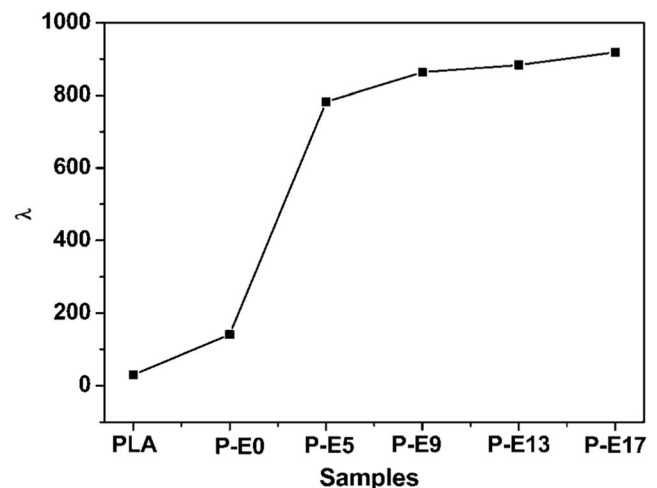
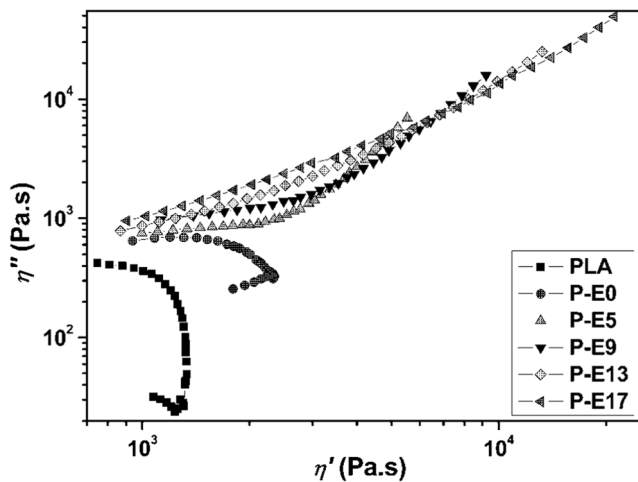


Fig. 8 Plots of relaxation time ( $\lambda$ ) versus MBS content



**Fig. 9** Cole–Cole plots of imaginary viscosity ( $\eta''$ ) versus real viscosity ( $\eta'$ ) for all samples

Table 3. Evidently, the  $E\alpha$  of PLA/EVOH blend with 9 phr MBS content was higher than those of PLA/EVOH blend without MBS content at the same weight loss except for weight loss of 10 and 40%. And the  $E\alpha$  of the P-E9 was higher than that of P-E0. The results indicated that the usage of MBS made degradation of PLA/EVOH blend more difficult.

**Oscillatory rheological analysis**

Figures 6(a) and (b) show the dependence of dynamic storage modulus ( $G'$ ) and complex viscosity ( $\eta^*$ ) for all samples, respectively. According to Fig. 6(a), with respect to  $G'$  of the PLA blended with EVOH alone that is, P-E0, it was higher

than that of neat PLA. It was also clearly observed that  $G'$  of the PLA/EVOH/MBS blend melts gradually increased with increasing MBS content, especially at low angular frequencies. These were due to the fact that the addition of MBS enhanced the melt elasticity and made the chain easier to entangle in the matrix. In other words, the entanglement density and melt elasticity of the PLA/EVOH/MBS blend were higher than those of the PLA/EVOH blend without MBS. However, the dependence of low-frequency  $G'$  on  $\omega$  weakens especially at high content levels. This indicated that the large scale polymer relaxations were restrained by the presence of MBS effectively.

As shown in Fig. 6(b), neat PLA and PLA/EVOH blend without MBS (P-E0) displayed a Newtonian liquid behavior at low angular frequencies. Moreover, P-E0 also showed a higher complex viscosity. For the PLA/EVOH/MBS blends, the low-frequency  $\eta^*$  increased with increasing MBS content. The increase in  $\eta^*$  of PLA/EVOH/MBS blends compared with PLA/EVOH blend at low angular frequencies range could be attributed to the increase of the interfacial adhesion between MBS and PLA, caused by the formation of entanglements between PLA chains and the grafted shell chains of MBS. The toughening effect (discussed in mechanical properties) was attributed to the energy dissipation caused by these tiny core-shell structure MBS particles having strong interfacial adhesion between the shell of MBS and the PLA matrix. In addition, the  $\eta^*$  of the PLA/EVOH/MBS blends showed a slight shear thinning at lower angular frequencies ( $< 10$  rad/s) and the shear thinning was more significant at higher angular frequencies (10~100 rad/s), which indicated that the blends had high melt strength and good processing mobility at higher angular frequencies.

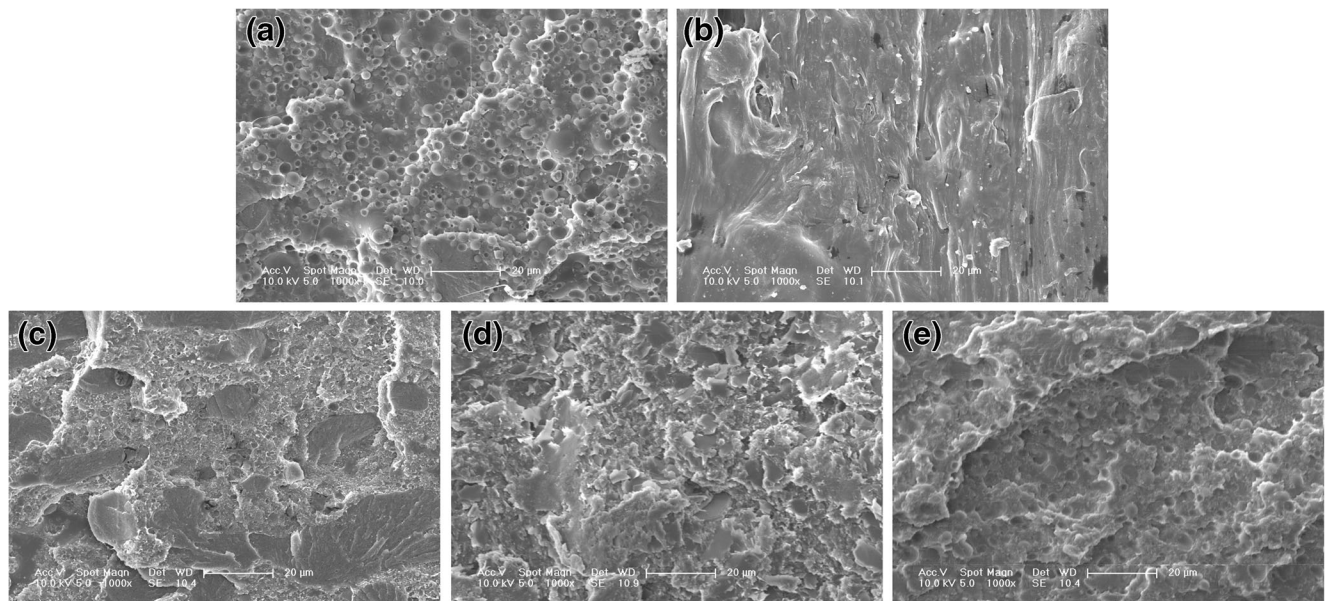


**Fig. 10** SEM micrographs of cryo-fractured surfaces of PLA/EVOH/MBS blends: **a** P-E0, **b** P-E5, **c** P-E9, **d** P-E13, **e** P-E17

## The Han and Cole–Cole analysis of rheological behavior

Figure 7 gives the Han plots of  $G' \sim G''$  for neat PLA and its blends. The curves of blends clearly present MBS content dependence. In addition, the reduced slope with the addition of MBS indicated that the blends became more heterogeneous. It was notable that the inflection point where the slope was shifted to a higher frequency with increasing MBS content. This indicated that much energy was necessary to change the degree of heterogeneity due to the increased physical association within the blends at a high content level. Those strong interactions and/or physical association between MBS and matrix changed the relaxation behavior of the PLA chain inevitably. The relaxation time ( $\lambda$ ) can be calculated as follows [28]:

$$\lambda = \frac{G'}{\eta^* \times \omega^2}$$

The calculated ratio of the relaxation time of all samples increased gradually with MBS content at the low angular frequency (0.1 rad/s), as shown in Fig. 8. It indicated that the role of MBS made the polymer chain need longer time for the relaxation became stronger with increasing loading levels. In other words, the presence of MBS highly restricted the chain mobility of PLA matrix.

The Cole–Cole plot is used to exhibit the imaginary viscosity ( $\eta''$ ) versus the real viscosity ( $\eta'$ ), where  $\eta' = G'/\omega$ ,  $\eta'' = G''/\omega$  [29–32]. It has been reported that the plot could be used to describe the viscoelasticity of distribution of relaxation time characteristic of heterogeneous polymer material and analyze the miscibility of polymer blend, and the curve could also reflect the existing network structure [33, 34]. The theoretical basis of Cole–Cole plot is Maxwell model. It is appropriate for describing the simple system of relaxation laws [29, 35, 36]. A smooth, semicircular shape of the plotted curves would suggest good compatibility, i.e., phase homogeneity in the melt, and any deviation from this shape shows a non-homogeneous dispersion and phase segregation due to immiscibility [32, 37, 38].

The Cole–Cole plots of all samples are shown in Fig. 9. As could be seen in Fig. 9, the differences of all samples were very clear. For neat PLA and PLA/EVOH blend, the Cole–Cole plots were close to a semicircle. However, addition of MBS showed an upward inflection, which might be indicative of poor compatibility or yield behavior. Moreover, the Cole–Cole plots of the PLA/EVOH/MBS blends showed more evident deviation at a high viscosity with increasing MBS content, indicating the long-term relaxation of those restrained PLA chains. The results were in agreement with the Han plots analysis.

## Phase behavior

The MBS also had an obvious effect on the morphology of the PLA/EVOH blends, as seen from the SEM images in Fig. 10. A poor interfacial adhesion was illustrated by the distinct interfaces between the matrix (PLA) and the dispersed sphere phase (EVOH) for the blends without MBS in Fig. 10a. The incorporation of 5 wt% MBS had evident influence on the phase morphology (Fig. 10b) and the surface was smooth. With increasing of MBS content, a clear phase-separated morphology was observed in Fig. 10(c)–(e). This was because high content of MBS might cause the particles agglomeration. Similar results has been studied in our previous research [24].

## Conclusions

The effect of MBS on the heat resistant, mechanical properties, thermal properties and rheological behavior of PLA/EVOH blends were investigated. The VST of neat PLA significantly increased from 66.8 °C to 159 °C after blending with 50 wt% EVOH. However, the VST was gradually decreased with increasing MBS content but was still much higher than that of neat PLA. The mechanical properties of PLA/EVOH blend was improved by incorporation of MBS. PLA/EVOH blend with 17 phr MBS showed the higher elongation at break (24.7%) and impact strength (10.1 kJ/m<sup>2</sup>), as were improved by 318 and 226%, respectively, when compared to that of PLA/EVOH blend without MBS. However, the tensile strength and elastic modulus for blends were gradually decreased with increasing MBS content. The TGA results suggested that PLA/EVOH/MBS blends were more stable than PLA/EVOH blend without MBS. With increasing MBS content, the  $G'$  and  $\eta^*$  increased at the measured temperatures, especially at low frequencies. The results of Han and Cole–Cole plots confirmed that chain mobility of PLA matrix was restricted.

**Acknowledgements** This work was supported by the fund of Science and Technology Bureau of Jilin Province of China (No. 20170204012SF), Chinese Science Academy (Changchun Branch) (No. 2017SYHZ0018 and No. 2017SYHZ0016), and the project National of Key Research and Development Program of China (No. 2016YFC0501402).

## References

1. Gross R, Kalra AB (2002) Biodegradable Polymers for the Environment. Science 297:803–807
2. Hu Y, Rogunova M, Topolkaev V, Hiltner A, Baer E (2003) Aging of poly(lactide)/poly(ethylene glycol) blends. Part 1. Poly(lactide) with low stereoregularity. Polymer 44:5701–5710
3. Bitinis N, Verdejo R, Cassagnau P, Lopez-Manchado MA (2011) Structure and properties of polylactide/natural rubber blends. Mater Chem Phys 129:823–831



4. Anderson KS, Hillmyer MA (2004) The influence of block copolymer microstructure on the toughness of compatibilized polylactide/polyethylene blends. *Polymer* 45:809–8823
5. Jonoobi M, Harun J, Mathew AP, Oksman K (2010) Mechanical properties of cellulose nanofiber (CNF) reinforced polylactic acid (PLA) prepared by twin screw extrusion. *Compos Sci Technol* 70: 1742–1747
6. Nampoothiri KM, Nair NR, John RP (2010) An overview of the recent developments in polylactide (PLA) research. *Bioresour Technol* 10:8493–8501
7. Balakrishnan H, Hassan A, Wahit MU, Yussuf AA, Razak SBA (2010) Novel toughened polylactic acid nanocomposite: mechanical, thermal and morphological properties. *Mater Des* 31:3289–3298
8. Liu MX, Zhang Y, Zhou CR (2013) Nanocomposites of halloysite and polylactide. *Appl Clay Sci* 75–76:52–59
9. Murariua M, Bonnauda L, Yoanna P, Fontaineb G, Bourbigotb S, Dubois P (2010) New trends in polylactide (PLA)-based materials: “Green” PLA-calcium sulfate (nano)composites tailored with flame retardant properties. *Polym Degrad Stab* 95:374–381
10. Lin S, Guo WN, Chen CY, Ma JL, Wang BB (2012) Mechanical properties and morphology of biodegradable poly(lactic acid)/poly (butylene adipate-co-terephthalate) blends compatibilized by transesterification. *Mater Des* 36:604–608
11. Meng QK, Hetzer M, Kee DD (2011) J Compos Mater PLA/clay/ wood nanocomposites: nanoclay effects on mechanical and thermal properties 45:1145–1158
12. Huda MS, Drzal LT, Misra M, Mohanty AK (2006) Wood-fiber-reinforced poly(lactic acid) composites: Evaluation of the physicomechanical and morphological properties. *J Appl Polym Sci* 102:4856–4869
13. Prakalathan K, Mohanty S, Nayak SK (2012) Polylactide/modified layered silicates nanocomposites: A critical analysis of morphological, mechanical and thermal properties. *J Reinf Plast Compos* 31: 1300–1310
14. Huda MS, Drzal LT, Mohanty AK, Mahanwar M (2006) Chopped glass and recycled newspaper as reinforcement fibers in injection molded poly(lactic acid) (PLA) composites: A comparative study. *Compos Sci Technol* 66:1813–1824
15. Nyambo C, Mohanty AK, Misra M (2011) Effect of Maleated Compatibilizer on Performance of PLA/Wheat Straw-Based Green Composites. *Macromol Mater Eng* 296:710–718
16. Nyambo C, Mohanty AK, Misra M (2010) Polylactide-Based Renewable Green Composites from Agricultural Residues and Their Hybrids. *Biomacromolecules* 11:1654–1660
17. Yu F, Liu T, Zhao X (2012) Effects of talc on the mechanical and thermal properties of polylactide. *J Appl Polym Sci* 125:E99–E109
18. Ray S, Yamada K, Okamoto M, Ueda K (2003) Biodegradable Polylactide/Montmorillonite Nanocomposites. *J Nanosci Nanotechnol* 3:503–510
19. Baltazar-y-jimenez A, Sain M (2012) Effect of bismaleimide reactive extrusion on the crystallinity and mechanical performance of poly(lactic acid) green composites. *J Appl Polym Sci* 124:3013–3023
20. Hashima K, Nishitsuji S, Inoue T (2010) Structure-properties of super-tough PLA alloy with excellent heat resistance. *Polymer* 51: 3934–3939
21. Nanda MR, Misra M, Mohanty AK (2011) The effects of process engineering on the performance of PLA and PHBV blends. *Macromol Mater Eng* 296:719–728
22. Liu MH, Yin Y, Fan ZP, Zheng XW, Shen S, Deng PY, Zheng CB, Teng H, Zhang WX (2012) The effects of gamma-irradiation on the structure, thermal resistance and mechanical properties of the PLA/EVOH blends. *Nucl Instr Meth Phys Res B* 274:139–144
23. Zhang HL, Liu NA, Ran XH, Han CY, Han LJ, Zhuang YG, Dong LS (2012) Toughening of polylactide by melt blending with methyl methacrylate-butadiene-styrene copolymer. *J Appl Polym Sci* 125: E550–E561
24. Yu T, Li R, Ren J (2009) Preparation and properties of short natural fiber reinforced poly(lactic acid) composites. *Trans Nonferrous Metals Soc China* 19:S651–S655
25. Ozawa T (1965) A new method of analyzing thermogravimetric data. *Bull Chem Soc Jpn* 38:1881–1886
26. Doyle CD (1961) Kinetic analysis of thermogravimetric data\*. *J Appl Polym Sci* 5:285–292
27. Wu DF, Wu L, Zhang M, Zhao YL (2008) Viscoelasticity and thermal stability of polylactide composites with various functionalized carbon nanotubes. *Polym Degrad Stab* 93:1577–1584
28. Chopra D, Kontopoulou M, Vlassopoulos D, Hatzikiriakos SG (2002) Effect of maleic anhydride content on the rheology and phase behavior of poly(styrene-co-maleic anhydride)/poly(methyl methacrylate) blends. *Rheol Acta* 41:10–24
29. Willoughby BG (2016) The Cole–Cole plot for cure: The cure and reversion of natural rubber. *J Appl Polym Sci* 133:44085-1–44085-9
30. Pu Z, Zheng P, Jia K, Liu X (2016) Effect of surface functionalization on the properties (rheological, mechanical, and dielectric) and microtopography of PEN/CPEN-*f*-CNTs nanocomposites. *Polym Compos* 37:2622–2631
31. Kwag H, Rana D, Cho K, Rhee J, Woo T, Lee BH, Choe S (2000) Binary blends of metallocene polyethylene with conventional polyolefins: rheological and morphological properties. *Polym Eng Sci* 40:1672–1681
32. Kovacs J, Dominkovics Z, Voros G, Pukanszky B (2008) Network formation in PP/Layered silicate nanocomposites: modeling and analysis of rheological properties. *Macromol Symp* 267:47–51
33. Wu DF, Wu L, Sun YR, Zhang M (2007) Rheological properties and crystallization behavior of multi-walled carbon nanotube/poly( $\epsilon$ -caprolactone) composites. *J Polym Sci B Polym Phys* 45: 3137–3147
34. Tian JH, Yu W, Zhou CX (2006) The preparation and rheology characterization of long chain branching polypropylene. *Polymer* 47:7962–7969
35. Cho K, Lee BH, Hwang KM, Lee H, Choe S (1998) Rheological and mechanical properties in polyethylene blends. *Polym Eng Sci* 38:1969–1975
36. Kim HK, Rana D, Kwag H, Choe S (2001) Melt rheology of ethylene 1-octene copolymer blends synthesized by Ziegler-Natta and metallocene catalysts. *Korea Polym J* 8:34–43
37. Han CD, Chuang HK (1985) Criteria for rheological compatibility of polymer blends. *J Appl Polym Sci* 30:4431–4454